Smashing Rays: Combining Realistic and Illustrative Visualization

Haysn Hornbeck* Usman R. Alim†

Department of Computer Science
University of Calgary

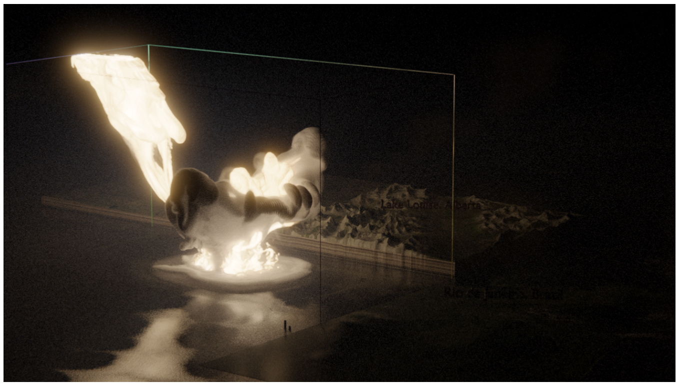

Figure 1: A still from the realistic version of the YA31 asteroid dataset. Rendered with 2,048 samples.

ABSTRACT

Traditional visualization techniques for volumetric datasets are excellent at revealing subtle details, but have difficulty conveying the physicality of a dataset. By using modern rendering techniques and physical models as a guideline, the authors attempt a visualization of an asteroid impact dataset which incorporates realism alongside illustrative techniques.

Index Terms: Human-centered computing—Scientific visualization—;——Computing methodologies—Ray tracing—; Computing methodologies—Scientific visualization——

1 INTRODUCTION

It is difficult to convey the dimensions of this dataset, depicts an asteroid crashing into the ocean. [1] Scale models are useful, but standard visualization techniques can create a disconnect. An X-ray of a broken bone excels at revealing subtle internal details, but lacks the visceral impact of a photograph. Similarly, the emissive gradients that are ubiquitous with volumetric datasets are useful illustrative tools yet intrinsically fail at conveying the physicality of the real world.

As computer graphics techniques have become more sophisticated and computers evolved to be more powerful, duplicating the appearance of real-world objects has become practical. For datasets which attempt to model the real world, as this one does, some effort should be made to present a realistic depiction of the event itself. By combining both illustrative and realistic rendering techniques, we should achieve better results than either alone.

2 PHYSICS

All substances radiate some form of electromagnetic radiation, as a by-product of molecular motion. The frequency and intensity of this "black-body" radiation primarily depends on the temperature and density of the substance, which can be modelled via Planck's Law.

2.1 Atmosphere

Including the Earth's atmosphere is essential for realism, as any emitted black-body radiation will scatter off it and generate a haze. Atmospheric attenuation is also critical for judging scale.

The appearance of Earth's atmosphere is primarily due to three separate phenomenon. Light scatters off the atom-scale molecules which make up the atmosphere, and this "Rayleigh scattering" depends only on the photon wavelength, plus particle size and density. Short wavelengths, greater size, and greater density increase the odds of a scattering event, but the probability distribution's shape is constant. The density of Earth's atmosphere follows a modified exponential decay curve, approximately $\rho(a) \approx 1.225 \cdot e^{-(.110 \cdot a)^{1.13}}$, where a is the altitude above the surface of the Earth in kilometres. This was generated by performing a curve-fit against a table drawn from a more complicated formula [9].

The second phenomena is aerosols such as dust, bacteria, and small water drops. These are approximately the same size as the wavelength of light they interact with. Internal reflections and phase cancellations result in a complicated "Mie scattering." It can be strongly effected by the wavelength of light, but the variance in particle sizes renders it near-achromatic.

These particles vary depending on the location on Earth and local weather conditions. For an isolated patch of ocean, aerosols would be thin and dominated by water vapour. The software package OPAC contains a database of common aerosol scattering functions, and its preset for clean maritime atmosphere was used [6]. Typically the aerosol component also follows an exponential decay, though with a steeper slope due to that component's heavier weight.

The third phenomenon is the ozone layer, which absorbs more light in the 550-650nm wavelengths than outside that band. [5]

2.2 Asteroid

The asteroid portion of the dataset consist primarily of basalt rock, with a density slightly higher than water and a melting point around 3,000 kelvin. Unfortunately, little is known of the optical properties at those temperatures. Fortunately, the milliseconds before impact are dominated by black-body radiation, due to the extreme heating of atmospheric entry, and after impact the rock is surrounded by a much greater volume of water. Treating it as a black-body with constant density is sufficient.

2.3 Clouds

While not as effective at conveying scale as more tangible objects like mountains and cities, clouds nonetheless contribute to the sense of realism. There is a sizable body of work on the real-time simulation of clouds [7]

Time constraints meant only common stratus clouds could be simulated. These exist at elevations between two and four kilometres.

---

*email: hhornbec@ucalgary.ca
†email: ualim@ucalgary.ca

They are formed when a warm, moist body of air rises into cooler parts of the atmosphere. As that air cools, water condenses out and forms small drops. In most cases these drops are small enough that Brownian motion and wind currents can keep them aloft indefinitely, and sparse enough that the odds them colliding and coalescing are low. If the original up-draft is strong enough, the droplet density and collision count may increase enough for gravity to become significant, leading to rain.

Surface tension plays a strong role in cloud physics. It prevents small drops from spontaneously forming without a "seed" to start the process, and bends water drops into a spherical shape. As the surface tension of water depends on temperature, the drop size distribution thus depends on water density and temperature [2].

2.4 Water

Some of the water ejected by the asteroid impact is hot enough to from steam, which has a much lower density and index of refraction than water, thus is more transparent. Materials with an index of refraction similar to the surrounding atmosphere rarely have a scattering function approaching that of a Dirac delta; instead, they have a gradually decreasing forward scatter that becomes uniform towards backscatter.

Studies of rain droplet distributions show that rainfall intensity and droplet size are proportionate, [11] implying very large drop sizes for airborne sea water. Fortunately, the interference effects that complicate Mie scattering decrease with drop size, and in this case can be ignored.

Surface tension decreases with temperature, and for water above 647 kelvin it reaches zero. In those conditions there is no barrier to condensation and no force pulling droplets to form spheres. Droplet sizes are better approximated by a Patero distribution, creating a scattering function that resembles a Dirac delta plus a Rayleigh distribution.

Conflicting scattering functions exist for ocean water, likely due to gas bubbles and particulate matter. Here, a smooth distribution was fitted to deep ocean samples from the Bahamas [10].

3 IMPLEMENTATION

Applying the aforementioned physics to the data was quite a challenge, given the small scale of the team. Rather than write a custom renderer, a stock release of Blender was used [3].

This introduced some complications, however. Cycles, Blender's path tracer, cannot handle volumes with varying indices of refraction, and workarounds that use geometry are unsatisfactory. This prevents the accurate simulation of the atmospheric lensing expected from hot air. The large scales involved mean that surface interactions contribute more to surface appearance, fortunately. The spray generated as aerodynamic drag tears apart the water surface will dominate, so droplet-based distributions should capture this well.

The asteroid dataset was converted to EXR format. Cycle's volume sampling settings are per-scene, so it was impossible to have good resolution of the simulation volume while also sampling the entire volumetric atmosphere; some compositing was necessary.

The sole example the authors could find of a renderer using arbitrary scattering functions was a custom version of the Mitsuba renderer [4]. Cycles does support the Henyey-Greenstein distribution, however, so we can build an arbitrary distribution from multiples of them. The node subsystem only allows distributions to be added, but the Open Shading Language subsystem also permits subtraction which improves the fit. Volume shaders were used extensively, relying on lookup tables to speed execution.

The subtle absorption of light due to the ozone layer was not simulated, as its millimetre-scale thickness would fail to integrate properly, and geometric solutions could introduce artefacts. The latest release of Blender also tends to artificially brighten the boundaries of volumes, and while development versions fixed this they proved too unstable to be relied on. Cycles may also fail to respect energy conservation when summing Henyey-Greenstein functions.

4 VISUALIZATIONS

The result was a two-minute thirty-second video; Figure 1 is a still from it with a boosted sample count. What follows are the major discoveries drawn from the video.

An astonishing amount of heat is generated in all the datasets. The maximum temperature is five times hotter than the surface of the Sun, and large volumes of water remain at Sun-like temperatures for much of the simulation. These are quite visible to any nearby wildlife, with minimal atmospheric blockage, and the pixel intensities suggest UV light at least five orders of magnitude greater than nominal; one second of exposure is worse than eighteen hours of continuous full-intensity sunlight.

If we overlay the states of water, we see the data dominated by liquid water but with a substantial amount of superheated steam, above the critical temperature.

Sudden changes in pressure are fatal to life. That cutoff is difficult to determine for sea life, but fish seem vulnerable to pressure increases of 4.8 atmospheres; [8] above the ocean, human fatalities begin with pressure deltas of 0.2 atmospheres. [12] If we overlay that on the dataset, every part of the simulated ocean experiences pressure changes in that range, sometimes more than once as the pressure wave reflects. The airborne shock wave is fatal for at least fifteen kilometres from the impact site, and can exceed one atmosphere at the front of the blast wave. The pressure is noticeably less in the direction of where the asteroid came from.

As for the magnitude of pressure difference from nominal, these did not extended beyond two orders of magnitude in the YA31 dataset.

REFERENCES

[1] The 2018 IEEE SciVis Contest.

[2] A. Bouthors, F. Neyret, N. Max, E. Bruneton, and C. Crassin. Interactive Multiple Anisotropic Scattering in Clouds. In *Proceedings of the 2008 Symposium on Interactive 3D Graphics and Games*, I3D '08, pp. 173–182. ACM, New York, NY, USA, 2008. doi: 10.1145/1342250.1342277

[3] B. Foundation. Blender Foundation.

[4] I. Gkioulekas, S. Zhao, K. Bala, T. Zickler, and A. Levin. Inverse volume rendering with material dictionaries. *ACM Transactions on Graphics (TOG)*, 32(6):162, 2013.

[5] J. Haber, M. Magnor, and H.-P. Seidel. Physically-based Simulation of Twilight Phenomena. *ACM Trans. Graph.*, 24(4):1353–1373, Oct. 2005. doi: 10.1145/1095878.1095884

[6] M. Hess, P. Koepke, and I. Schult. Optical Properties of Aerosols and Clouds: The Software Package OPAC. *Bulletin of the American Meteorological Society*, 79(5):831–844, May 1998. doi: 10.1175/1520-0477(1998)079<0831:OPOAAC>2.0.CO;2

[7] R. Hufnagel and M. Held. A Survey of Cloud Lighting and Rendering Techniques. *Journal of WSCG*, p. 12.

[8] J. A. Lewis. Effects of underwater explosions on life in the sea. Technical report, DEFENCE SCIENCE AND TECHNOLOGY ORGANIZATION CANBERRA (AUSTRALIA), 1996.

[9] R. Minzner. The 1976 standard atmosphere and its relationship to earlier standards. *Reviews of geophysics*, 15(3):375–384, 1977.

[10] T. J. Petzold. Volume scattering functions for selected ocean waters. Technical report, Scripps Institution of Oceanography La Jolla Ca Visibility Lab, 1972.

[11] D. SempereTorres, J. M. Porr, and J.-D. Creutin. Experimental evidence of a general description for raindrop size distribution properties. *Journal of Geophysical Research: Atmospheres*, 103(D2):1785–1797. doi: 10.1029/97JD02065

[12] R. K. Zipf and K. L. Cashdollar. Effects of blast pressure on structures and the human body. 2006.